

Interacting Supernovae: Types IIn and Ibn

Nathan Smith

Abstract Supernovae that show evidence of strong shock interaction between their ejecta and pre-existing, slower circumstellar material (CSM) constitute an interesting, diverse, and still poorly understood category of explosive transients. The chief reason that they are extremely interesting is because they tell us that in a subset of stellar deaths, the progenitor star may become wildly unstable in the years, decades, or centuries before explosion. This is something that has not been included in standard stellar evolution models, but may significantly change the end product and yield of that evolution and complicates our attempts to map SNe to their progenitors. Another reason they are interesting is because CSM interaction is a very efficient engine for making bright transients, allowing super-luminous transients to arise from normal SN explosion energies, and allowing transients of normal supernova luminosities to arise from sub-energetic explosions or low radioactivity yield. CSM interaction shrouds the fast ejecta in bright shock emission, obscuring our normal view of the underlying explosion, and the radiation hydrodynamics of the interaction is challenging to model. The CSM interaction may also be highly non-spherical, perhaps linked to binary interaction in the progenitor system. In some cases, these complications make it difficult to definitively tell the difference between a core collapse or thermonuclear explosion, or to discern between a non-terminal eruption, failed supernova, or weak supernova. Efforts to uncover the physical parameters of individual events and connections to possible progenitor stars make this a rapidly evolving topic that continues to challenge paradigms of stellar evolution.

Nathan Smith
Steward Observatory, University of Arizona, 933 N. Cherry Ave., Tucson, AZ 85721, USA, e-mail:
nathans@as.arizona.edu

1 Introduction

Type II_n superovae (SNe II_n hereafter), defined broadly as SNe that exhibit bright and narrow Balmer lines of H in their spectra, were recognized as a distinct class of objects relatively late compared to other SN subtypes (see Schlegel 1990 and Filippenko 1997 for early background). This was spurned largely by observations of the classic SN II_n 1988Z and connecting it to unusual properties in some other SNe. Our understanding of this class and various subclasses has been evolving continuously since then as more SNe are discovered and the diversity of SNe II_n grows. The related class of SNe Ib_n, showing narrow lines of He in the optical spectrum (and relatively weak H lines), was clearly identified only 10 years ago following studies of the prototype SN 2006jc (Pastorello et al. 20017; Foley et al. 2007).

Interpreting observations of interacting SNe is fundamentally different from studying “normal” SNe. For our purposes here, “normal” SNe are those cases where the observed emission comes from a photosphere receding (in mass coordinates) back through freely expanding SN ejecta, or radiation from the optically thin SN ejecta at late times that are heated internally by radioactivity. These are the main subtypes of II-P, II-L, IIb, Ib, Ic, Ic-BL discussed elsewhere in this volume. SNe II_n and Ib_n represent a physically very different scenario, where the usual diagnostics and physical pictures cannot be applied. As a means of introduction to the topic, we begin with two warnings that should be heeded when thinking of SNe II_n and related subtypes of interacting SNe:

Warning 1. The main engine is conversion of kinetic energy to light in a shock at the outside boundary of the SN. It is not shock-deposited energy leaking out of a homologously expanding envelope (as in early phases of a SN II-P), nor is it internal heating from radioactive decay (most SNe at peak and at late times). Instead, the observed radiation comes primarily from a shock crashing into dense CSM which - unfortunately from the point of view of predictive models - makes the situation complicated and malleable. “Malleable” here means that it is hard to calculate predictive models because the shock luminosity can rise and fall somewhat arbitrarily depending on the radial density structure of the CSM. One should not take the absence of normal signatures (broad lines in the SN ejecta photosphere or nebular emission lines) as an indication that these are not true SNe, because CSM interaction can mask these normal signatures. Moreover, radiation from the shock can propagate back into the SN ejecta, changing their appearance.

Warning 2. SNe II_n and related categories are not really a *supernova type* (or more accurately, not an intrinsic explosion type), but an *external phenomenon* associated with CSM interaction. Any type of core collapse or thermonuclear SN (or for that matter, any non-SN explosive outflow) can appear as a SN II_n

or SN Ibn. All that is required is fast ejecta with sufficient energy crashing into slower ejecta with sufficient density. This is a cause of much confusion and uncertainty.

As a consequence of these differences compared to other SNe, we find a very diverse range of properties in interacting SNe. There is not a singular evolutionary path that leads to an interacting SN, nor is there a singular mapping of SNe IIn to a specific progenitor type. For example, we usually associate SNe II-P as coming from moderately massive red supergiants of 8-20 M_{\odot} (Smartt 2009), but such assignments are not so straightforward for SNe IIn. It can be difficult to tell the difference between a SN IIn that arises from the core collapse of a very massive luminous blue variable (LBV) or LBV-like star, and a thermonuclear explosion of a white dwarf with dense CSM. SNe IIn can arise any time there is dense H-rich material sitting around a star that explodes, which might happen in a number of different ways. Exploring this diversity in progenitors as well as in CSM and explosion properties is a main emphasis of current work because it has important implications for mass loss and instability in the late phases of stellar evolution.

The detailed physical picture and time evolution of interacting SNe may also be very different from normal SNe. Instead of a more-or-less spherical photosphere receding through outflowing ejecta, we have radiation from a thin shell, which may start out as an optically thick sphere, but may transition to a limb-brightened shell that is transparent in the middle and optically thick at the edges. We may have underlying explosions that would otherwise be too faint to be observed (for example, explosions producing very low radioactive yield), and that don't contribute to the traditional populations of extragalactic SNe, but nevertheless yield bright transients through their CSM interaction. Thus, we should be mindful that some SNe IIn may be powered by entirely new (or so far observationally unrecognized) classes of explosions other than SNe II-P, II-L, IIb, Ib, and Ic. Much of this is still little explored or uncharted territory.

For this chapter, it is also worth making a distinction of scope. Actually, all SNe are interacting with surrounding material at some level, because space is not a true vacuum and an interaction arises naturally even when fast SN ejecta expand into low density ISM or their progenitor's normal wind (this eventually forms a standard SN remnant). Whether this can be detected in extragalactic SNe shortly after explosion — and in what waveband it is detected — depends to a large extent on the CSM density. For the purposes of discussion here, we take “Interacting SNe” to mean those with extraordinarily strong CSM interaction that leads to a radiative shock at early times after explosion, producing narrow lines in the visible-wavelength spectrum and enhanced optical continuum luminosity at early times. We exclude otherwise normal SNe that show signs of interaction based on radio or X-ray emission, although it should be kept in mind that these represent the tail of a continuum of CSM density stretching from superluminous SNe, through more traditional SNe IIn, and on to lower CSM density.

2 Basic Physical Picture

When a SN explodes inside a dense cocoon of CSM, a strong shock is driven into the CSM, creating a basic structure as depicted in Figure 1. A forward shock (FS) is driven outward into the CSM, and a corresponding reverse shock (RS) is driven back into the SN ejecta. In the simplest picture, four zones are delineated where heated material can radiate and contribute to the observed spectrum:

- Zone 1. The unshocked CSM outside the forward shock (photoionized).
- Zone 2. The swept-up CSM that has been hit by the forward shock.
- Zone 3. The decelerated SN ejecta that have encountered the reverse shock.
- Zone 4. The freely expanding SN ejecta.

In normal SNe, we only see emission from Zone 4 at visible wavelengths as the photosphere recedes back through the freely expanding ejecta, creating broad emission and absorption lines whose velocities decrease smoothly with time as the

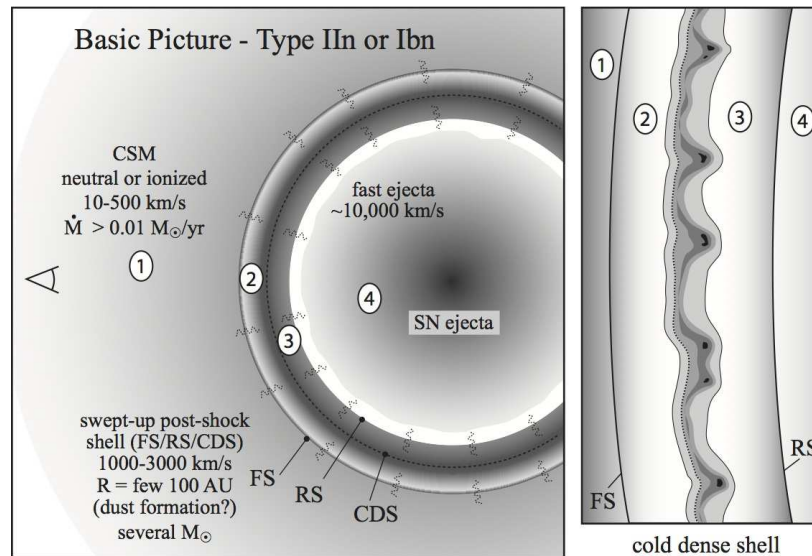


Fig. 1 Sketch of the basic picture in CSM interacting SNe. Four different zones are noted with numbers: (1) the pre-shock CSM, (2) the shocked CSM, (3) the shocked SN ejecta, and (4) the freely expanding SN ejecta. These zones are divided by boundaries corresponding to the **forward shock**, the **reverse shock**, and the **contact discontinuity** between the shocked CSM and shocked ejecta where material cools, mixes via Rayleigh-Taylor instabilities, and piles up. This is often called the **cold dense shell (CDS)** in a SN II_n or Ib_n. The squiggly radial lines are meant as a reminder that X-rays and UV radiation generated in the shock can propagate out to the CSM or inward to the unshocked ejecta, changing the physical state of the gas there. A zoom-in of zones 2 and 3 is shown at the right. In practice, efficient radiative cooling can cause these two zones to collapse to very thin layers, and mixing can make them merge into one thin clumpy shell. This figure is adapted from Smith et al. (2008).

emitting layer recedes through the monotonic outflow. Zones 2 and 3 are sometimes detected in X-rays or radio emission if the CSM is dense enough. Zone 1 might be seen in absorption lines, although this is rare.

In an interacting SN, any of these 4 zones can contribute strongly to the emitted visible-wavelength spectrum. In fact, the continuum photosphere moves through all 4 zones as time proceeds, and their relative contributions to line emission change with time. The basic picture of this interaction, which can differ widely in detail from case to case, has been described many times in the literature (Chugai 1997, 2001; Chugai & Danziger 1994; Chugai et al. 2004; Smith et al. 2008, 2010a, 2015; Dessart et al. 2015).

At early times, radiation from the shock propagates upstream and causes an ionized precursor. At this stage (sometimes only lasting a day or two, sometimes several weeks or months), the electron scattering continuum photosphere is actually in the unshocked CSM, obstructing our view of the shock. The spectrum usually appears as a smooth blue continuum with narrow emission lines that have broad Lorentzian wings. These wings are not caused by Doppler motion of shocked gas, but by electron scattering as narrow line photons work their way out of the optically thick CSM.

As the pre-shock CSM density drops at larger radii, eventually the photosphere recedes into zones 2 and 3, and we begin to see a transformation in the spectrum. This usually occurs around the time of peak luminosity. Strong intermediate-width (few 10^3 km s^{-1}) components of permitted lines appear, sometimes accompanied by P Cygni absorption. Here we are seeing radiation from the post-shock gas. Because of strong radiative cooling (which occurs by definition in an interacting SN), Zones 2 and 3 can collapse into a geometrically very thin layer, and mixing at the contact discontinuity may cause these two zones to merge. The standard picture is that this cooled gas is very dense and piles up in a “cold dense shell” (Chugai et al. 2004). This gas is continually reheated by the shock, and emits strongly in lines like H α or He I that appear as the strongest intermediate-width lines in the spectra of SNe II n and Ib n , respectively. This line emission continues to be strong even after the continuum photosphere recedes further, because the CDS is reheated by X-ray and UV radiation from the FS and RS.

After peak, the continuum photosphere may recede back into Zone 4 in the freely expanding SN ejecta. If the CSM interaction is relatively weak or shortlived, an observer might then see a fairly normal SN spectrum with broad P Cygni lines at the end of the photospheric phase, or typical signatures of SN ejecta heated by radioactive decay in the nebular phase. However, if CSM interaction is strong and sustained, an observer might never actually see a normal SN ejecta photosphere or nebular phase, and the P Cygni absorption may be filled in. The underlying SN (heated by the original shock deposition or radioactive decay) may fade in a few months, whereas CSM interaction might remain very bright for many months or years. How long this CSM interaction stays bright is determined mainly by the duration and speed of the pre-SN mass loss, not by the explosion. By the time the CSM fades enough to become transparent, the inner SN ejecta may be too faint to detect on their own, and the ongoing CSM interaction may continue to dominate

the spectrum at late times. In fact, the fast SN ejecta may be heated predominantly by radiation from the CSM interaction shock that propagates backward into the outermost ejecta, creating a very different time dependent spectrum than is seen in a normal SN heated from the inside-out by radioactive decay. One must bear these differences in mind when interpreting SNe IIn spectra, especially at late phases.

Of course, if the geometry is asymmetric, any of these zones can be seen simultaneously and at different characteristic velocities, potentially making the interpretation quite complicated. Absorption features may or may not be seen, depending on viewing angle. Even if the interaction is spherically symmetric, we might see multiple zones simultaneously because long path lengths through the limb-brightened edges of the CDS may remain optically thick while material along our line of sight in the CDS has already become transparent. Very strong and non-monotonic changes in density and velocity make this a complicated situation that presents a significant challenge for radiation transfer codes. For the time being, unraveling the various clues in the spectral evolution is something of an art form.

The total luminosity generated by CSM interaction in this picture can be high because a radiative shock is a very efficient engine to convert kinetic energy into visible-wavelength light. Whereas a normal SN II might have a total radiated energy that is 1% of its kinetic energy, a Type II SN can have a total radiated energy closer to 50% or more of the total explosion kinetic energy. The luminosity of CSM interaction L depends essentially on the rate at which CSM mass is entering the forward shock, which of course depends mostly on the progenitor's mass loss rate, and is typically expressed as

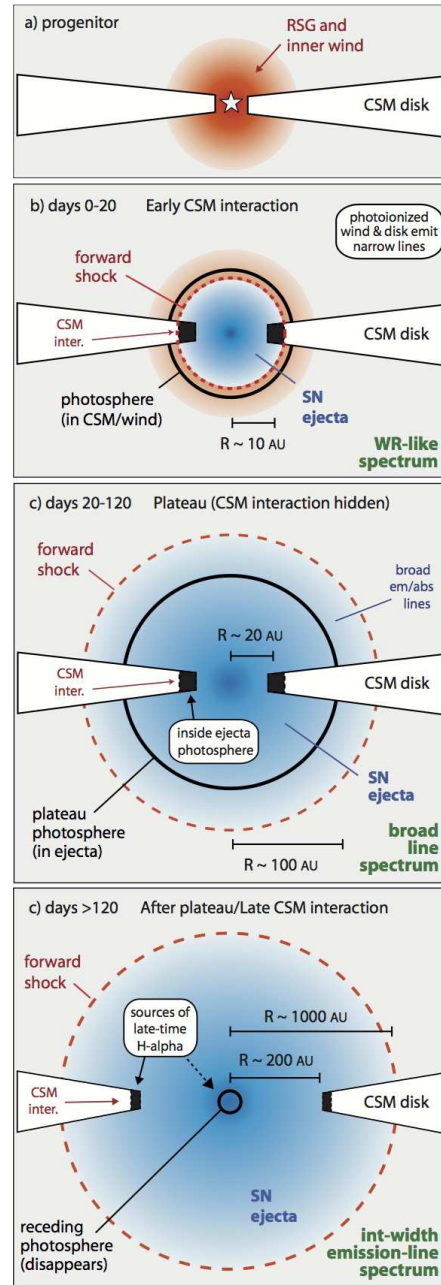
$$L = \frac{1}{2} w V_{\text{CDS}}^3, \quad (1)$$

where w is the wind density parameter $w = 4\pi R^2 \dot{\rho}$, or $w = \dot{M}/V_{\text{CSM}}$, and V_{CDS} is the value for the evolving speed of the CDS. From the intermediate-width lines in optical spectra we can measure the value of V_{CDS} (be careful not to do this at early times when electron scattering in the CSM is determining the line width; at early times the true value of V_{CDS} is hidden from the observer, and it may be much higher than when it is seen at later times). We can also measure V_{CSM} from the narrow component due to pre-shock gas, especially if a narrow P Cygni profile is observed (note here that higher resolution spectra with $R \simeq 4000$ are especially useful). Using the luminosity (L) derived from photometry (note that for V and R bands, the bolometric correction may be quite small if the apparent temperature is around 6000-7000 K), we can then turn this equation around to estimate the progenitor star's mass-loss rate

$$\dot{M}_{\text{CSM}} = 2 L \frac{V_{\text{CSM}}}{(V_{\text{CDS}})^3}, \quad (2)$$

that occurred at some time $t=t_{\text{exp}}(V_{\text{CDS}}/V_{\text{CSM}})$ in the past, where t_{exp} is the time after explosion to which these measurements correspond (careful again, as t_{exp} has its own potentially large uncertainties).

Fig. 2 Sketch of the more complicated interaction when the CSM is highly asymmetric; in this example a disk-like distribution surrounds the progenitor. (a) The initial pre-explosion state is a progenitor with a wind, as well as a dense disk at radii of ~ 10 AU. (b) Immediately after explosion, narrow lines may arise either from a photoionized dense wind or from the disk. Strong CSM interaction with the disk occurs immediately and enhances the early luminosity, but the emergent spectrum may be dominated by narrow lines with Lorentzian wings. (c) CSM interaction with the disk has slowed the forward shock in the equatorial plane, but the SN ejecta expand relatively unimpeded in the less dense polar regions. After a few days, the normal SN ejecta photosphere may expand so much that it completely envelops the CSM interaction occurring in the disk. The enveloped CSM interaction can now heat the optically thick ejecta from the inside and contribute significantly to the total visible luminosity, even if no narrow lines are seen, and may cause the photosphere to be asymmetric. (d) At late times, the SN ejecta photosphere recedes. At this time, the CSM interaction in the disk is exposed again (now with larger radial velocities because it has been accelerated), and intermediate-width and possibly doubled-peaked lines may be seen from the ongoing interaction. This sketch was originally invoked to explain the observed evolution of PTF11iqb (Smith et al. 2015).



This sort of analysis is oversimplified, but it is sufficient to give us a ballpark idea of the sorts of mass-loss rates that are required to produce a Type II_n supernova. In order to make the CSM-interaction luminosity high enough that it can compete with the photosphere of a typical SN (say $3 \times 10^8 L_{\odot}$, or -16.5 mag), and with representative values of $V_{\text{CSM}} = 100 \text{ km s}^{-1}$ and $V_{\text{CDS}} = 2500 \text{ km s}^{-1}$, we require a huge mass-loss rate of order $0.01 M_{\odot} \text{ yr}^{-1}$. SNe II_n tend to be more luminous than -16.5 mag, or even super-luminous, and so the implied mass-loss rates get very big (although remember that V_{CDS} is probably faster than 2500 km s^{-1} in the early optically thick phases near peak). This mass-loss rate is well beyond the realm of normal stellar winds (Smith 2014). We return to the implications for progenitors later.

For a constant mass-loss rate in the progenitor wind (and hence, a single value of w), L will usually drop with time as the forward shock decelerates. Equation (1) does a pretty good job of describing the visible continuum luminosity as long as the material is optically thick enough to reprocess most or all of the X-ray and UV luminosity into visible continuum radiation. It doesn't work so well at very early times during the rise or at peak when diffusion is important, and it doesn't work at later times when the X-rays begin to leak out and the $H\alpha$ line emission becomes very strong. At these phases, Equation (2) will underestimate the required progenitor mass-loss rate if L is derived from the visible light curve. At later times, one needs to adopt a very uncertain efficiency factor in order to derive physical parameters from observations. The efficiency of converting kinetic energy into visible light can vary widely depending on CSM density (van Marle et al. 2010), CSM composition (H-free gas tends to be more transparent), and geometry, as discussed next.

3 A (Probably) More Realistic Physical Picture

Figure 1 is a good place to begin when picturing the physics of CSM interaction, but it may be something of a fantasy. One exceedingly obvious result from 20 years of *Hubble Space Telescope* imaging of circumstellar shells is that they are often not spherically symmetric, and this is especially true of massive stars and eruptive mass loss. Bipolar shells and equatorial disks or rings are common around evolved massive stars.

This has an impact on our interpretation of observed signatures of CSM interaction, because when spherical symmetry is broken, it can affect the qualitative appearance of the spectrum, and it can change line profile shapes. More importantly, it can dramatically change the inferred total energy and mass budgets, and sometimes it can hide evidence of CSM interaction altogether. If one assumes spherical symmetry in an interacting SN that is actually not spherically symmetric, one can be led to astoundingly wrong conclusions. In this case, the “simplest” assumptions may be simply inappropriate.

Figure 2 shows an example of how the scenario in Figure 1 might be modified if a SN is surrounded by an equatorial disk-like distribution of CSM as opposed

to a spherical shell (this is borrowed from Smith et al. 2015, where much of this topic is discussed in more detail). A key point is that if the dense CSM is disk-like, then strong CSM interaction only occurs in a small fraction of the total solid angle involving the equatorial regions (see Mauerhan et al. 2014; Smith et al. 2014). The vast majority of the SN ejecta (say, 90% if the disk only intercepts 10% of the solid angle seen by the SN) can expand unimpeded in the polar directions. Thus, as far as the majority of the SN ejecta are concerned, their kinetic energy is not tapped by CSM interaction, and they would emit a normal broad-lined spectrum. For the unlucky 10% of the SN ejecta in the equator, their kinetic energy is converted into heat and radiation by the shock. In this way, CSM interaction with a disk can create SNe that are overluminous compared to normal SNe II-P, for example, but not nearly as luminous as the class of super-luminous SNe. This may be applicable to many SNe IIn.

Enveloped, Swallowed, and Hidden CSM Interaction. There is a nonintuitive but very interesting result that can occur from interaction with asymmetric CSM, which is that *the resulting SN might not show any narrow lines even if much of its luminosity comes from strong CSM interaction*. This can occur in the following way: Imagine that a SN progenitor is surrounded by a dense CSM disk located at a radius 10-20 AU. The initial shock interaction might produce strong narrow lines in the first few days. In the disk, the fast SN ejecta are decelerated, creating a strong shock that produces a moderately high luminosity and bright narrow-line emission from this CSM interaction. However, the remaining 90% of the SN ejecta expand unimpeded as if there was no CSM interaction. The normal SN ejecta photosphere quickly expands to a radius of 10s of AU in a few days. At such time, the optically thick SN ejecta can completely envelope the equatorial CSM interaction, hiding some or all of the narrow and intermediate-width lines that arise due to CSM interaction. The extra radiated energy generated by the equatorial CSM interaction is now unable to escape freely because it has been swallowed by the opaque fast ejecta, and this radiative energy is instead deposited in the interior of the optically thick SN ejecta and must diffuse out. It will therefore add extra heat to the outer envelope, perhaps mimicking extra deposition of radioactive decay energy. The asymmetric injection of heat in this way will likely make the photosphere asymmetric. Viewed from the outside at a time of roughly a month after explosion, one might then observe a broad-lined SN photosphere with enhanced luminosity and perhaps a longer than normal duration, unusual line profiles, or significant polarization. At this stage, it would be difficult to tell the difference between some small extra amount of radioactive heating or buried CSM interaction.

All hope is not lost, though, because an observer might then be able to deduce that CSM interaction was contributing to the main light curve all along by watching until late times. After the SN recombination photosphere recedes, the enveloped CSM interaction region is exposed once again. When this happens, the dense CSM disk that has been swept up into a cold dense shell (or cold dense torus) and accelerated to a few thousand km s^{-1} may now be seen again via strong intermediate-width line emission. Prominent examples of this are SN 1998S, PTF 11iqb, SN 2009ip, and even the SN IIfb 1993J (Leonard et al. 2000; Pozzo et al. 2004; Smith et al.

2014, 2015; Mauerhan et al. 2014; Matheson et al. 2000). This line emission can be much stronger than the nebular emission from the optically thin inner ejecta heated by the dwindling radioactive decay. Moreover, the ongoing CSM interaction can emit strong X-rays that propagate back into the SN ejecta, potentially changing the emergent nebular spectrum.

Perhaps the most important thing to realize is that we now have two different physical explanations for the wide diversity in peak luminosity of SNe IIn, even if all explosions have the same 10^{51} ergs of kinetic energy. The range of luminosity from the strongest CSM interaction in super-luminous SNe down to cases with minimal extra luminosity provided by CSM interaction can be explained either by ramping down the density of the progenitor’s wind, or by increasing the degree of asymmetry in dense CSM. The strongest clues that significant CSM asymmetry is present are from: (1) spectropolarimetry (e.g., Mauerhan et al. 2014), (2) asymmetric line profile shapes (although some asymmetry can also be caused by dust or occultation by the SN photosphere itself), or (3) the time evolution of velocities (for example, seeing very fast speeds in the SN ejecta that persist after the strongest CSM interaction has subsided; Smith et al. 2014). The last point confirms unequivocally that not all the fast SN ejecta participated in the CSM interaction. There may also be some special observed signatures of asymmetry at certain viewing angles (edge-on, for example) and specific times. If one does recognize such signatures of asymmetry, one must realize that the progenitor mass-loss rate inferred from equation (2) as well as the SN explosion energy are not just lower limits, but likely underestimates by a factor of ~ 10 . Of course, one can also invoke differences in explosion energy, explosion mechanism, SN ejecta mass, and radioactive yield to also contribute to the observed diversity.

4 Observed Subtypes

The main physical parameters that determine the observed properties of a typical core-collapse SN are the mass of ejecta, kinetic energy of the explosion (as well as the mass of synthesized radioactive material), and the composition and structure of the star’s envelope at the time of explosion. This leads to the wide diversity in observed types of normal ejecta-dominated core-collapse SNe and thermonuclear SNe (II-P, II-L, IIb, Ib, Ic, Ia).

For interacting SNe, we have all these same free parameters of the underlying explosion, as well as the possibility of SNe with low or no radioactive yield and a wider potential range of explosion energy — but to these we must also add the variable parameters associated with the CSM into which the SN ejecta crash: CSM mass and/or mass-loss rate, radial distribution (speed and ejection time before explosion), CSM composition, and CSM geometry. Given these parameters, it may not be surprising that the class of interacting SNe is extremely diverse, and observations are continually uncovering new or apparently unique characteristics. Moreover, a SN can change type depending on when it is seen. An object that looks like a SN IIn

in the first few days can morph into a normal SN II-L or IIb if it undergoes enveloped/asymmetric CSM interaction, and may then return to being a Type IIc at late times, as discussed in the previous section.

There are, however, some emerging trends among interacting SNe. The list below attempts to capture some of these emerging subtypes among interacting SNe that appear to share some common and distinct traits. The reader should be advised, however, that this is still a rapidly developing field, so this is neither a definitive nor a complete list, and moreover, there are observed events that seem to skirt boundaries or overlap fully between different subtypes. Further subdivisions are likely to be clarified with time. The list below includes a descriptive name and some prototypical or representative observed examples that are often mentioned (again, not a complete list).

Superluminous IIc; compact shell (SN 2006gy). SN 2006gy was the first superluminous SN to be discovered, and it remains extremely unusual even though several other SLSNe IIc have since been found (see Smith et al. 2007, 2010a; Ofek et al. 2007; Woosley et al. 2007). It had a slow rise to peak (~ 70 days) and faded within another 150 days or so, which is unlike the other SLSNe IIc that seem to fade very slowly and steadily from peak. Also unusual was that it had strong intermediate-width P Cygni absorption features in its spectra, strong line-blanketing absorption in the blue, and narrow P Cygni features from the CSM. It is thought to have arisen from a relatively compact and opaque CSM shell, where CSM interaction mostly subsided within a year. In this case, the CSM is thought to have arisen from a single eruption that ejected $\sim 20 M_{\odot}$ about 8 years prior to core collapse (Smith et al. 2010a). SN 2006gy is one of the best observed SNe IIc and is often discussed, but readers should be aware that it is not at all typical.

Superluminous IIc; extended shell (SN 2006tf, SN 2010jl, SN 2003ma). These are basically the superluminous version of the SN 1988Z-like subclass, discussed next. Unlike SN 2006gy, they show strong, smooth blue continua without much line blanketing, and little or no P Cygni absorption in their intermediate-width lines. They also tend to fade slowly and steadily, in some cases remaining bright for several years as the shock runs through an extended dense shell (e.g., Smith et al. 2008; Rest et al. 2011; Fransson et al. 2014).

Enduring IIc (SN 1988Z, SN 2005ip). These SNe IIc show a smooth blue continuum superposed with strong narrow and intermediate-width H lines, and in some cases even broad components (Chugai & Danziger 1994; Aretxaga et al. 1999; Smith et al. 2009). Some cases, such as SN 2005ip, have strong narrow coronal emission lines (Smith et al. 2009), implying photoionization of dense clumpy CSM by X-rays generated in the shock. They tend to be more luminous than SNe II-P, but not as bright as SLSNe. These objects tend to fade very slowly and show signs of strong CSM interaction for years or even decades after discovery; SN 1988Z is *still* going strong. One can picture these as a stretched-out version of the SLSNe IIc, in the sense that they have somewhat lower luminosities at peak, but they last longer, eventually sweeping through similar amounts of total CSM mass (of order several

to $20 M_{\odot}$). While SLSNe have CSM that is so dense that it requires eruptive LBV-like mass loss in the years or decades before explosion, these enduring SNe IIn like SN 1988Z and SN 2005ip can potentially be explained by extreme RSG winds blowing for centuries before core collapse. If there is such a thing as a “standard” SN IIn, this is probably what most IIn-enthusiasts have in mind.

Transitional IIn (SN 1998S, PTF11iqb, SN 2013cu). This class of SNe IIn only shows fleeting signatures of CSM interaction that disappear quickly, and may be entirely missed if the SN isn’t discovered early after explosion. SN 1998S was one of the nearest and best studied SNe IIn that helped shape our understanding of SNe IIn, and so it has often been referred to as “prototypical” – but it really isn’t. SN 1998S wasn’t very luminous and its spectral signatures of CSM interaction disappeared pretty quickly, transitioning into a broad-lined ejecta-dominated photosphere within a couple weeks (Leonard et al. 2000; Shivvers et al. 2015). This indicated that the total mass of CSM was actually quite modest (of order $0.1 M_{\odot}$ or so), substantially different from the types noted above. If it had not been caught so early, SN 1998S might not have been classified as a Type IIn at all. An older example of this was SN 1983K (Niemela et al. 1985). More recently, a few other related objects have been found (SN 2013cu & PTF11iqb; Gal-Yam et al. 2014; Smith et al. 2015), which only showed a Type IIn spectrum for the first few days after discovery (and these cases were thought to have been discovered very early; within 1 day or so of explosion). PTF11iqb and SN 2013cu then morphed into broad lined SNe with spectra similar to SNe II-L or IIb, respectively. At late times, PTF11iqb showed strong CSM interaction again, very similar to SN 1998S and the Type IIb SN 1993J. We do not know how common these are. While SNe IIn represent roughly 8-9% of core collapse SNe (Smith et al. 2011), this statistic does not include SNe that only exhibit Type IIn characteristics for a brief window of time and then morph into other types after a few days; thus, early strong CSM interaction with dense inner winds might be fairly common among the larger population of ccSNe. The corresponding (potentially very important) implication is that many core collapse SNe may suffer a brief pulse of episodic mass loss shortly before core collapse. The reason for this is not yet known, but is probably related to the final nuclear burning stages and may have important implications for models of core collapse.

Late-time interaction in otherwise normal SNe (SN 1993J, SN 1986J). The overlap with the previous subclass is probably considerable, but it is worth mentioning that some otherwise normal SNe (perhaps appearing normal simply because we missed the early IIn signatures in the first day or so) show particularly strong CSM interaction at late times. Some of the more common cases are SNe IIb and SNe II-L, for which there are well-studied and famous nearby examples like SN 1993J and SN 1986J (Matheson et al. 2000; Milisavljevic & Fesen 2013). For these, the transition from a SN into a SN remnant is somewhat blurry, and some of these are well known nearby aging SNe. Because this interaction is most apparent when the SNe have faded after the first year, this phenomenon can only be studied in nearby galaxies. These may be caused by strong RSG winds, or by equatorial CSM deposited by binary interaction in objects like SNe IIb that are more clearly associated with the

end products of binary evolution. The reason why this CSM still resides close to the star at the time of death is still unclear, and (as for the previous subclass) may hint at some rapid and dramatic changes in the final nuclear burning sequences in a wider fraction of SN progenitors than just standard SNe IIn.

Delayed onset, slow rise, multi-peaked (SN 2009ip, SN 2010mc, SN 2008iy, SN 1961V, SN 2014C). In contrast to the previous subclass, some SNe IIn show little or no signs of CSM interaction at first, but then rise to the peak of CSM interaction after a delay of months or years. This delay is presumably due to the time it takes for the fastest SN ejecta to catch up to a CSM shell that was ejected a year or more before core collapse. The underlying SN ejecta photosphere could be relatively faint at first if the progenitor was a more compact BSG, like SN 1987A, or an LBV; the faintness of the initial SN might cause the initial transient to be missed altogether, or mistaken as a pre-SN eruption rather than the actual SN, since it might precede the delayed onset of peak luminosity that actually arises when the ejecta overtake the CSM. It must be admitted, however, that from the time of peak onward, these tend to appear as relatively normal SNe IIn; as such, the distinction between this “delayed onset” subclass and other SNe IIn might be artificial, and only distinguishable in cases with fortuitous pre-discovery or pre-peak data. The amount of delay in the onset of CSM interaction bears important physical information about the elapsed time between the pre-SN eruption and core collapse. In the case of SN 2009ip, the delay of ~ 40 days made sense, as fast SN ejecta caught up to CSM moving at 10% the speed, associated with eruptions that were actually observed a year or so before the SN (Mauerhan et al. 2013a, 2014; Smith et al. 2014). SN 1961V had a light curve consistent with a normal SN II-P for the first ~ 100 days, followed by a brighter peak (Smith et al. 2011b). In SN 2014C, the delayed onset had different chemical properties, where a H-poor stripped-envelope SN crashed into a H-rich shell after a year (Milisavljevic et al. 2015). In some cases, however, the delayed onset is rather extreme and the CSM interaction strong; SN 2008iy appeared to be a relatively normal core collapse SN in terms of luminosity, which rose to very luminous peak as a Type IIn after 400 days (Miller et al. 2010). SN 1987A might be thought of as an even more extended version of this, where the onset of CSM interaction was delayed for 10 years as the SN ejecta caught up to CSM ejected $\sim 10^4$ yr earlier. We don’t know what fraction of normal SNe have a delayed onset of CSM interaction, since most SNe are not monitored continuously with large telescopes for years or decades after they fade.

Type IIn-P (SN 1994W, SN 2011ht, the Crab). This is a distinct subclass of SNe IIn that exhibit IIn spectra throughout their evolution, but have light curves with a well-defined plateau drop (Mauerhan et al. 2013b). They are not to be confused with “transitional” SNe IIn/II-P that may have narrow lines at early times and evolve into an otherwise normal SN II-P. In SNe IIn-P, the narrow H lines with strong narrow P Cyg profiles are seen for the duration of their bright phase. The drop from the plateau is quite extreme (several magnitudes) and the late-time luminosities suggest low yields of ^{56}Ni . These may be the result of $\sim 10^{50}$ erg electron capture SN explosions with strong CSM interaction (Mauerhan et al. 2013b; Smith

2013). It has been proposed that the Crab Nebula may be the remnant of this type of event, although this remains uncertain (Smith 2013).

SN IIn impostors (LBVs, SN 2008S-like, etc.). These transients have narrow H lines in their spectra similar to SNe IIn, but are subluminous (fainter than $M_R \simeq -15.5$ mag), and have slower velocities than normal SNe IIn (see Smith et al. 2011b and references therein). One may argue that the luminosity cut is arbitrary, but the narrow lines without any broad wings do seem distinct from other SNe IIn (most of the time). Some are certainly non-terminal transients akin to LBVs (because they repeat or the star survives), but some cases are not so clear. Although they may not be SNe, they are included here because we’re not sure yet — some objects thrown into this bin could be underluminous because they are interacting transients that arise from “failed” SNe (fallback to a black hole), pulsational pair instability SNe, ecSNe, SNe from compact BSG progenitors with low radioactive yield, mergers with compact object companions, or other terminal events.

Type Ia/IIn or Ia-CSM (SN 2002ic, SN 2005gj, PTF11kx). These are transients that show spectral features indicative of an underlying SN Ia ejecta photosphere, but with strong superposed narrow H lines and additional continuum luminosity (Silverman et al. 2013). Cases with stronger CSM interaction tend to obscure the Type Ia signatures, leading to ongoing controversy about their potential core collapse or thermonuclear nature (Benetti et al. 2006). Cases with weaker CSM interaction (PTF11kx) reveal the Type Ia signatures more clearly, allowing them to be identified unambiguously as thermonuclear events. The relatively rare evolutionary circumstance that leads a thermonuclear SN to have a large mass of H-rich CSM is still unclear.

Type Ibn (SN 2006jc). These are similar to SNe IIn, except that H lines are weak or absent, so that narrow or intermediate-width He I lines dominate the spectrum ($H\alpha$ is weaker than He I $\lambda 5876$). Without the assistance of H opacity, these objects tend to fade more quickly than most SNe IIn. The class is quite diverse and includes a range of H line strengths and CSM speeds, including transitional IIn/Ibn cases (SN 2011hw) where H and He I lines have similar strength (Smith et al. 2012; Pastorello et al. 2008, 2015). It has been hypothesized that the likely progenitors may be Wolf-Rayet stars or LBVs in transition to a WR-like state (Pastorello et al. 2007; Foley et al. 2007; Smith et al. 2012).

Type Icn (hypothetical). A discovery of this class has not yet been reported (as far as the author is aware), but as transient searches continue, there may be cases where a SN interacts with a dense shell of CSM that is both H and He depleted, yielding narrow or intermediate-width lines of CNO elements, for example. With sufficient creativity, one can imagine stellar evolution pathways that might create this; such SNe are clearly rare, and if they never turn up, their absence will provide interesting physical constraints for some binary models.

5 Dust Formation in CSM interaction

The formation of dust by SNe may be essential to explain the amount of dust inferred in high redshift galaxies. SNe with strong CSM interaction provide an avenue for dust formation that is different from normal SNe, and possibly much more efficient. In normal SNe, dust forms in the freely expanding ejecta where there is a competition between cooling to low enough temperatures while the ejecta are also rapidly expanding and achieving lower and lower densities. Even if dust forms efficiently, this ejecta dust might get destroyed when it crosses the reverse shock. In interacting SNe, by contrast, evidence suggests that dust can form very rapidly in the extremely dense, post-shock cooling layers (zones 2 and 3 in Figure 1). Moreover, this dust is already behind the shock and may therefore stand a better chance of surviving and contributing to the ISM dust budget.

The first well-studied case of post shock dust formation was in SN 2006jc, which was a Type Ibn. The classic signs of dust formation were seen starting at only 50 days post-discovery, in an increase in the rate of fading, excess IR emission, and an increasing blueshifted asymmetry in emission-line profiles (Smith et al. 2008b). The last point strongly favored post-shock dust formation, since this was seen in the intermediate-width lines that were emitted from the post-shock zones. The Type Ibn event may have been the result of a Type Ic explosion crashing into a He-rich shell. In this case, one might think that the C-rich ejecta were important in assisting the efficient formation of dust, as is seen for the post-shock dust formation in colliding-wind WC+O binaries (Gehrz & Hackwell 1974; Williams et al. 1990). However, similar evidence for this same mode of post-shock dust formation has also been seen in several Type IIn events, such as SN 2005ip, SN 1998S, SN 2006tf, SN 2010jl, and others (Smith et al. 2008a, 2009, 2012; Fox et al. 2009; Gall et al. 2014; Pozzo et al. 2004). It may therefore be the case that enhanced post shock dust formation is a common outcome of strong CSM interaction, where efficient post-shock cooling causes the forward shock to collapse and become very dense.

6 Progenitors and Pre-SN Mass Loss

Basic considerations about powering SNe IIn with CSM interaction, noted above, argue that extremely strong pre-SN mass loss is required. What sorts of progenitor stars can give rise to this dense CSM?

6.1 CSM Properties

The first thing to do is to look around us in the nearby universe and ask what sort of observed classes of stars might fit the bill. Figure 3 makes this comparison by plotting the diversity in wind density of interacting SNe, deduced from the pre-

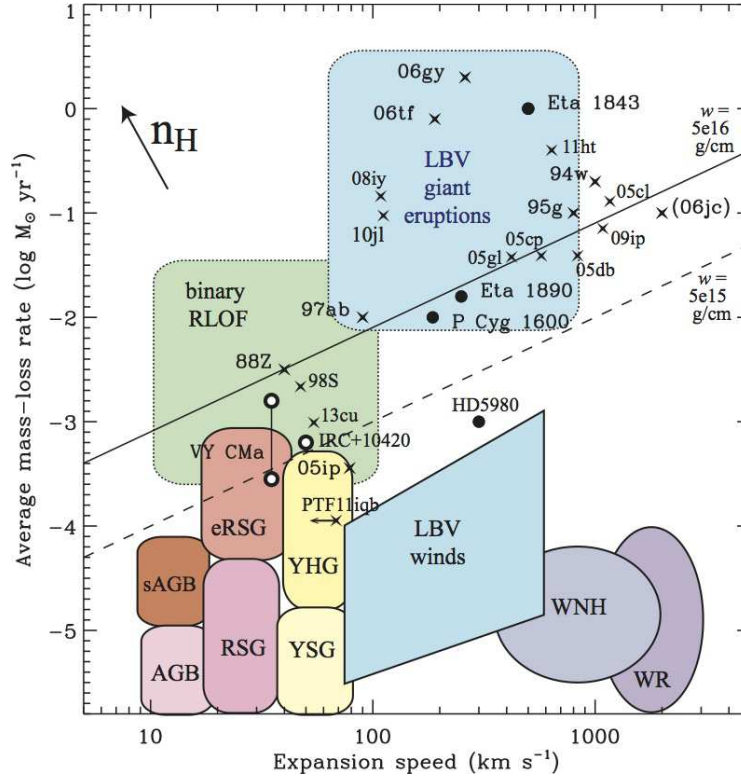


Fig. 3 Plot of mass-loss rate as a function of wind velocity, comparing values for interacting SNe to those of known types of stars. The solid colored regions correspond to values for various types of evolved massive stars taken from the review about mass-loss by Smith (2014), corresponding to AGB and super-AGB stars, red supergiants (RSGs) and extreme RSGs (eRSG), yellow supergiants (YSG), yellow hypergiants (YHG), LBV winds and LBV giant eruptions, binary Roche-lobe overflow (RLOF), luminous WN stars with hydrogen (WNH), and H-free WN and WC Wolf-Rayet (WR) stars. A few individual stars with well-determined very high mass-loss rates are shown with circles (VY CMa, IRC+10420, η Car's eruptions, and P Cyg's eruption). Also shown with X's are some representative examples of SNe IIn (and one SN Ibn) that have observational estimates of the pre-shock CSM speed from the narrow emission component as measured in moderately high resolution spectra as well as estimates of the progenitor mass-loss required, taken from the literature. The diagonal lines are wind density parameters ($w=M/V_{\text{CSM}}$) of 5×10^{16} and 5×10^{15} g cm^{-1} , which are typically the lowest wind densities required to make a SN IIn. Values are taken from the literature; this figure is from a paper in prep. by the author. Note that in some cases, an observationally derived value for the mass of the CSM has been converted to a mass-loss rate with a rough estimate of the time elapsed since ejection.

shock wind (or shell) expansion speed and the inferred mass-loss rate, as compared to expected mass-loss from known types of stars. The shaded and colored regions in this figure show rough parameters for different classes of evolved massive stars that are potential SN progenitors with strong winds. These are taken from the recent review by Smith (2014); see the caption for definitions. In this plot, a given wind

density parameter (required for a particular value of a CSM interaction luminosity via Equation 1) has a diagonal line increasing to the upper right. The solid line shows a typical value for a moderate-luminosity SN IIn, and the dashed line is a typical lower bound for wind densities required to make a SN IIn (although an object can be slightly below this line and still make a Type IIn spectrum if the wind is clumpy or asymmetric).

We can see immediately that the normal classes of evolved stars with strong but relatively steady winds (WR stars, LBV winds, normal YSGs and RSGs, AGB stars) do not match up to the wind density required for SNe IIn. These could potentially produce SNe that have strong X-ray or radio emission from CSM interaction, but they are not dense enough to slow the forward shock, and to cause the forward shock to cool radiatively and collapse into the cool dense shell that is required for intermediate-width $H\alpha$. The only observed classes of stars that have the high wind densities required are the giant eruptions of LBVs and the most extreme cool hypergiants (the slower winds of extreme RSGs and YHG make their winds have density comparable to the shells in LBV giant eruptions, even though the mass-loss rates are lower). Both classes of stars are not steady winds, but rather, they are dominated by relatively short-lived phases of eruptive or episodic mass loss, or extreme dense and clumpy winds. In the case of LBVs, these are eruptions that last a few months to a decade. For extreme RSGs and YHGs, these are phases of enhanced mass loss that may persist for centuries to a few thousand years.

From the point of view of their mass loss, LBVs (and to a lesser extent the most extreme cool hypergiants) are good candidates for the progenitors of SNe IIn. This does not, however, mean that these stars are necessarily all poised to explode in the next couple years, nor does it mean that they are the only possible IIn progenitors. The caveat is that the progenitors of SNe IIn undergo strong eruptive or episodic mass loss immediately before core collapse, and may therefore experience significant changes in their internal structure. The stars may have looked very different in the time period before their pre-SN eruptions began. Hence, these stars in their immediate pre-SN state may not actually exist among nearby populations of stars in the Milky Way and Magellanic Clouds right now.

Also note that this is a mass-loss *rate*, not total mass, and note that these are usually lower limits to the required mass-loss rate (the high rate makes high optical depths, and hence, makes an observational determination difficult). In cases where we have estimates of the total mass ejected, one must divide by an assumed timescale to derive a mass-loss rate; for SNe IIn, this timescale is inferred from the relative velocities of the CSM and CDS. Since we are essentially plotting a wind density, it is important to recognize that two different SNe with the same inferred progenitor mass-loss rate might have had that high mass loss lasting for very different amounts of time, and hence, may have very different amounts of total mass ejected shortly before the SN. In some cases, the total mass can be more constrainting than the rate. For example, the total mass of $\sim 20 M_{\odot}$ required for some superluminous SNe IIn rules out any progenitor stars with initial masses below about $30\text{-}40 M_{\odot}$, because we need a comparable mass of SN ejecta to provide enough momentum for a long-lasting interaction phase (not to mention mass loss due to winds

throughout the life of the star). Also, there are cases like SN 2005ip where the inferred mass-loss rate is on the low end, but this SN had remarkably long-lasting CSM interaction that suggests a total mass of order $15 M_{\odot}$ of H-rich material (e.g., Smith et al. 2009; Stritzinger et al. 2012), which rules out lower-mass RSGs and super-AGB stars for its progenitor.

Warning 3. One must be somewhat cautious in drawing conclusions about the progenitor based on only the observed pre-shock CSM speed. We generally think of the outflow speed being proportional to the star’s escape velocity, so we expect slower outflows from RSGs and YHG, somewhat faster speeds for LBVs and BSGs (few 10^2 km s^{-1}), and very fast outflows for WR stars (few 10^3 km s^{-1}). This is a good guide if the outflow is a relatively steady radiation-driven wind. However, remember that the observed CSM may be the result of eruptive or explosive mass loss driven by a shock wave. If so, it is possible to get a relatively fast outflow even from a bloated RSG; eruption speeds need not match steady wind speeds for various types of stars in Figure 3. Moreover, the high luminosity of the SN itself can potentially accelerate the pre-shock CSM (essentially a radiatively driven wind from a temporarily much more luminous star), which could also lead to a faster pre-shock CSM speed than expected for a certain type of star, or multiple velocity components in the CSM.

6.2 Direct Detections

The types of inferences described above are all still based on rather indirect and circumstantial evidence. A potentially more direct way to link SNe to their progenitors is to detect the progenitor star in pre-explosion imaging data, usually with the *Hubble Space Telescope*, although ground-based imaging has been used for some very nearby cases (see review by Smartt 2009). This method has been used successfully for some other types of SNe, especially SNe II-P, IIb, and one particularly famous II-pec event that occurred 20 years ago. The progenitor identification can be confirmed after the SN fades, to verify that the progenitor star is gone (as opposed to being a chance alignment, a host cluster, or a companion star).

For interacting SNe, however, the interpretation of pre-SN direct detections can be a little tricky. First, the “direct” detection of the progenitor might actually be a direct detection of a pre-SN eruption and not the quiescent star. This source might indeed fade after the SN, but it is hard to tell if the star is really dead, or if the eruption has just subsided and the star returned to its quiescent state. Inferring an initial mass by comparison with stellar evolution tracks is also complicated if the progenitor might be in an outburst rather than in its quiescent state (we don’t have much choice here and are lucky if there is even one *HST* image in the archive, but one just needs to be aware of the caveat). A second complication is that some

SNe IIn have persistent CSM interaction for years or decades after the SN, and so one might need to wait a very long time before the SN has faded enough to be fainter than the progenitor. Third, a faint progenitor or even a faint upper limit to a progenitor is very inconclusive in terms of its implication for the mass of the star. This is because with interacting SNe, there is, by definition, a large mass of CSM. Thus, we certainly expect some cases where the progenitor was surrounded by a massive dust shell that should obscure the progenitor star’s visible light output. This makes it difficult to place a progenitor detection (or upper limit) on an HR Diagram and infer an initial mass if one has only an optical filter.

Despite this ambiguity, there have been a few lucky and important cases that guide our intuition about the progenitors of SNe IIn and SNe Ibn.

SN 2005gl: This was a SN IIn where a very luminous progenitor consistent with an LBV star like P Cygni was detected in *HST* imaging and the SN had an implied mass-loss rate of $0.01 M_{\odot} \text{ yr}^{-1}$ (Gal-Yam et al. 2007), and this source then faded after the SN (Gal-Yam & Leonard 2009). Moreover, the pre-shock CSM speed of 420 km s^{-1} inferred from narrow H lines was suggestive of the fast outflow from an LBV (Smith et al. 2010). As noted above, there is some ambiguity as to whether the pre-SN detection was a massive quiescent LBV-like star or a pre-SN eruption caught by the *HST* image. In either case an eruptive LBV-like star is likely, although the implied initial mass may be different. Based on its spectral evolution, SN 2005gl fits into the subclass of “transitional” SNe IIn like SN 1998S and PTF11qib, which show a Type IIn spectrum at first, but later show broad P Cygni lines indicative of a SN photosphere, so this can be taken as an argument that it was most likely a core-collapse SN event.

SN 1961V: Long considered an extreme LBV or SN impostor event, recent arguments favor an actual core-collapse SN for the 1961 transient (Kochanek et al. 2011; Smith et al. 2011). If this was a SN, then it has one of the best documented progenitor detections and progenitor variability among SNe, and it holds the record for the most massive directly detected SN progenitor. The pre-1961 variability suggests a very massive $\sim 100 M_{\odot}$ blue LBV-like progenitor that was variable before the SN. The source at the SN position is now more than 5.5 mag fainter than this progenitor (a much more dramatic drop than in the case of SN 2005gl), and there is no IR source with a luminosity comparable to the progenitor (Kochanek et al. 2011), so the extremely massive star is likely dead.

SN 2006jc: An eruption in 2004 was noted as a possible LBV or SN impostor, and then a SN occurred at the same position 2 years later. The pre-SN outburst had a peak luminosity similar to SN impostors (Pastorello et al. 2007). The SN explosion two years later was of Type Ibn with strong narrow He I emission lines (Foley et al. 2007, Pastorello et al. 2007). There is no detection of the quiescent progenitor, but this unusual case implies an LBV-like eruption that occurred in a WR-like progenitor star that was clearly H depleted. The CSM speed was of order 1000 km s^{-1} , which is consistent with WR stars, and faster than typical LBVs.

SN2011ht: This belongs to the subclass of SNe IIn-P, which are thought to arise from lower-energy explosions that may be linked to electron capture SNe in 8-10 M_{\odot} super-AGB stars (Mauerhan et al. 2013b; Smith 2013). There is no detection of

the quiescent progenitor, although deep upper limits seem to rule out a luminous, blue quiescent star (Mauerhan et al. 2013b; Roming et al. 2012). However, Fraser et al. (2015) reported the detection of pre-SN eruption activity in archival data. This may be an important demonstration that non-LBVs can have violent pre-SN eruptions as well.

SN 2010jl: This was a SLSN IIn with roughly $10 M_{\odot}$ or more of CSM. Smith et al. (2011c) identified a source at the location of the SN in pre-explosion HST images that suggested either an extremely massive progenitor star or a very young massive-star cluster; in either case it seems likely that the progenitor had an initial mass above $30 M_{\odot}$. We are still waiting for this SN to fade to see if the progenitor candidate was actually the progenitor or a massive young cluster/association.

SN 2009ip: This source was initially discovered as an LBV-like outburst in 2009 (its namesake) before finally exploding as a much brighter SN in 2012. A quiescent progenitor star was detected in archival HST data, indicating a very massive 50-80 M_{\odot} progenitor (Smith et al. 2010b, Foley et al. 2011). In this case, the *HST* detection may well have been the quiescent progenitor, rather than an outburst, because much brighter outbursts came later. It showed slow variability consistent with an S Dor LBV-like episode (Smith et al. 2010b), followed by a series of brief LBV-like giant eruptions (Smith et al. 2010b, Mauerhan et al. 2013a, Pastorello et al. 2013). Unlike any other object, we also have detailed, high-quality spectra of the pre-SN eruptions (Smith et al. 2010b, Foley et al. 2011). The presumably final SN explosion of SN 2009ip in 2012 would fall into the “delayed onset” subclass, since at first the fainter transient showed very broad lines indicative of a SN photosphere. Reaching peak, however, it looked like a normal SN IIn, as the fast ejecta crashed into the slow material ejected 1-3 years earlier (Mauerhan et al. 2013a, Smith et al. 2014). A number of detailed studies of the bright 2012 transient have now been published, although there has been some controversy about whether the 2012 event was a core-collapse SN (Mauerhan et al. 2013a; Ofek et al. 2013; Prieto et al. 2013; Smith et al. 2014) or some type of extremely bright nonterminal event (Fraser et al. 2013a, Pastorello et al. 2013, Margutti et al. 2014). More recently, Smith et al. (2014) showed that the object continues to fade, and its late-time emission is consistent with late-time CSM interaction in normal SNe IIn. If SN 2009ip was indeed a SN, it provides a strong case that very massive stars above $30 M_{\odot}$ may in fact experience core collapse and explode, and that LBV-like stars are linked to some SNe IIn.

6.3 Links to Progenitor Types

We will undoubtedly find more examples of direct detections and pre-SN outbursts in the future. One must bear in mind, though, that LBVs and eruptive precursors are relatively easy to detect because they are brighter than any quiescent stars, so these cases do not rule out alternatives such as dust-enshrouded RSGs, or faint and hot quiescent stars. From various clues described above such as the CSM mass and mass-loss rate, CSM expansion speed, H-rich composition, and direct detections of

progenitors or environments, we can attempt to link certain subclasses of interacting SNe to different possible progenitors. Some associations are more likely than others.

SLSN II_n (compact and extended shell; SN 2006gy or SN 2010jl-like): Based on the extreme required masses of (10-20 M_{\odot}) of H-rich CSM, typically expanding at a few hundred km s⁻¹, it seems very likely that the progenitors of SLSNe II_n are very massive, eruptive LBV-like stars (see review by Smith 2014). If they are not truly LBVs, then they do a very good impersonation. The simple fact that very massive stars above $\sim 40 M_{\odot}$ are exploding as H-rich SNe is a challenge to understand, since stellar evolution models predict all those stars to shed their H envelopes at roughly solar metallicity. Most of these have huge mass ejections occurring just a few years or decades before the SN, so the connection to nearby LBVs — some of which have shells that are hundreds or thousands of years old — is not yet clear. LBV-like progenitors are even likely in cases where the progenitor is optically faint, if a pre-SN eruption has obscured the star with a dust cocoon (as is likely to be the case, given the consequent CSM interaction). Since the progenitors must be very massive stars simply because of the mass budget, the physical mechanism of pulsational pair instability eruptions is a viable candidate for the pre-SN outbursts (Woosley et al. 2007). This is not the case for the remainder of SNe II_n, because they are too common (Smith et al. 2014).

Normal, enduring SNe II_n (SN1988Z-like): Likely progenitor types are LBVs or extreme cool hypergiants (YHG/eRSGs), based mostly on the required mass-loss rates and observed CSM speeds. For these enduring cases, we require either strong mass loss in several centuries preceding the SN, or a large bipolar shell ejected shortly before the SN with a range of ejection speeds (to accommodate CSM interaction over a large range of radii, lasting for a long time). Total CSM masses that exceed 10 M_{\odot} in some cases and integrated radiated energies that exceed 10⁵¹ ergs (over years) point to relatively massive progenitor stars. Enhanced late-phase RSG mass loss (Yoon & Cantiello 2010) or instabilities in late nuclear burning sequences (Quataert & Shiode 2012; Smith & Arnett 2014) are good candidates for the episodic mass-loss.

Transitional or fleeting SNe II_n (SN 1998S-like): Likely progenitors are RSGs, YHG, or BSG/LBVs with less extreme pre-SN bursts of mass loss, confined to a relatively short-duration event preceding core collapse (i.e. within a few years preceding the SN). These objects also seem to require highly asymmetric CSM interaction, to allow the expanding SN photosphere to completely or mostly envelope the disk of CSM interaction that emits narrow lines (as discussed in Section 3). For this reason, there is a strong suspicion that close binary interaction plays a role in their pre-SN episodic mass loss, although it must still be linked somehow to the final nuclear burning sequences (see Smith & Arnett 2014 regarding the role of close binaries in this scenario).

SNe II_n-P (SN 2011ht-like): The favored scenario for these events involves an intermediate-mass progenitor in a super-AGB phase that suffers a sub-energetic (10⁵⁰ erg) electron-capture SN. This is based on the low ⁵⁶Ni yield, the deep absorption features that imply more-or-less spherical symmetry, and the energy/mass budgets inferred (Mauerhan et al. 2013b; Smith 2013). However, observations can-

not yet confidently rule out a more massive progenitor that suffers fallback to a black hole, yielding a smaller ejecta mass and very low ^{56}Ni yield (although in the case of SN 2011ht, progenitor upper limits seem to argue against this interpretation). This type of SN also fits the bill for SN 1054 and the Crab nebula, whose abundances and kinetic energy seem to point to an electron capture SN from an intermediate-mass star (Nomoto et al. 1982). If these are ecSNe, then the pre-SN episodic mass-loss might be related to nuclear flashes in the advanced degenerate core burning sequences.

SN IIn impostors: This group of putatively non-SN transients may be quite diverse, and it may include transients that have narrow lines because they are powered largely by CSM interaction (and weaker explosions than core-collapse SNe) and other transients that have narrow lines because they have slow winds/outflows. This may include LBVs, super AGB stars, binaries with a compact object, stellar mergers, pre-SN nuclear burning instabilities, failed SNe, or all of the above. Any massive supergiant star enshrouded in dust or with strong binary interaction that suffers an instability is a viable candidate. The theoretical mechanisms for this class of outbursts is still very poorly understood, and there is probably considerable overlap with pre-SN outbursts that lead to SNe IIn and Ibn.

SNe Ibn: The most likely progenitors are massive WR stars that for unknown reasons undergo pre-SN outbursts. This is interesting, because there is no known precedent for an observed eruption in a H-deficient massive star.

SNe Ia/IIn or Ia-CSM: If these really are thermonuclear SNe Ia (some cases seem clear, others are still debated in the literature), then the exploding progenitors are white dwarfs that have arisen from initial masses below roughly $8 M_{\odot}$. In this case, a single degenerate system is clearly required to supply the large mass of H-rich CSM (several M_{\odot} in some cases). There is, as yet, no viable explanation for the sudden ejection of a large mass of H (by the companion) shortly preceding the thermonuclear explosion of the WD.

7 Closing comments

Observations of interacting SNe present one of the most interesting challenges to our understanding of the end phases of evolution for massive stars. What makes these stars explode before they explode? Computational resources are only beginning to meet the needs of the complex problem of simulating convection and nuclear burning coupled with stellar structure and turbulence in these final phases (Arnett & Meakin 2011; Meakin & Arnett 2007). The fact that $\sim 10\%$ of core-collapse events are preceded by some major reorganization of the stellar structure and energy budget tells us that we have been missing something important, which might be a key ingredient for understanding core collapse SNe more generally. It will be important to try and understand if this 10% corresponds to the most extreme manifestation of a wider instability (for example, if all stars undergo some instability in the final burning sequences, but only the most extreme cases lead to detectably violent mass loss

and SNe IIn) or if SNe IIn are the outcome of special circumstances in a particular evolution channel (i.e. interacting binaries within a certain mass and orbital period range). There is still very little information available on any trends with metallicity, although this is always good to investigate when mass loss plays a critical role.

Recent years have seen something of a paradigm shift in massive star studies. Formerly standard or straightforward assumptions about the simplicity of single-star evolution are giving way to more complicated scenarios as astronomers grudgingly admit that binary stars not only exist, but are common and influential (e.g., Sana et al. 2012). This may be especially true among transient sources and stellar deaths that seem otherwise peculiar or difficult to understand. Given the very high multiplicity fraction among massive stars, binary interaction should probably not be considered a last resort or the refuge for an uncreative theorist, but rather, a default assumption.

Whether they are binaries or not, all SNe IIn require some major shift in stellar structure and mass loss before the SN. The synchronization with core collapse gives a strong implication that something wild is happening in the latest sequences of nuclear burning. Those cases where a star changes its structure as a result of these nuclear burning instabilities (i.e. an inflated envelope) in a close binary system seem promising for inducing sudden eruptive behavior for various reasons (Smith & Arnett 2014). Single stars may also be able to induce their own violent mass loss in the couple years preceding core collapse due to energy transported to the envelope from Ne and O burning zones (Quataert & Shiode 2012). However, we do not yet have a good explanation in single-star evolution for the strong mass-loss that leads to the “enduring” class of SNe IIn or some of the more extreme cases of “delayed onset” of CSM interaction, where the strong interaction that lasts for years after explosion suggests very strong mass loss for *decades or centuries* before core collapse. If binary interaction is an important ingredient, then this sort of interaction before a SN might make asymmetric CSM very common, suggesting that we should be paying close attention to possible observed signatures of asymmetry.

Acknowledgements My attempt to understand interacting SNe and their connections to massive stars has benefitted greatly from conversations with numerous people, but especially Dave Arnett, Matteo Cantiello, Nick Chugai, Selma de Mink, Ori Fox, Morgan Fraser, Dan Kasen, Jon Mauerhan, Stan Owocki, Jose Prieto, Eliot Quataert, Jorick Vink, and Stan Woosley. While drafting this chapter, I received support from NSF grants AST-1312221 and AST-1515559.

Cross-References

1. Supernova of 1054 and its Remnant, the Crab Nebula
2. Observational and Physical Classification of Supernovae
3. Supernovae from super AGB Stars (8-12 Msun)
4. Supernovae from massive Stars (12-100 Msun)
5. Very Massive and Supermassive Stars: Evolution and Fate
6. Progenitor of SN 1987A
7. Supernova Progenitors Observed with HST
8. Interacting Supernovae and the Influence on Spectra and Light Curves
9. X-ray and radio emission from circumstellar interaction

10. Dust and Molecular Formation in Supernovae
11. Supernova remnant from SN1987A
12. The Supernova - Supernova Remnant Connection

References

1. Aretxaga I, Benetti S, Terlevich RJ, Fabian AC, Cappellaro E, Turatto M, et al. 1999, MNRAS, 309, 343
2. Arnett WD, & Meakin C. 2011, ApJ, 741, 33
3. Benetti S, Cappellaro E, Turatto M, Tautenberger S, Haratyunyan A, Valenti S. 2006, ApJ, 653, L129
4. Chugai NN. 1997, Ap&SS, 252, 225
5. Chugai NN. 2001, MNRAS, 326, 1448
6. Chugai NN, & Danziger IJ. 1994, MNRAS, 268, 173
7. Chugai NN, Blinnikov SI, Cumming RJ, Lundqvist P, Bragaglia A, Filippenko AV, et al. 2004, MNRAS, 352, 1213
8. Dessart L, Audi E, Hillier DJ. 2015, MNRAS, 449, 4304
9. Filippenko AV. 1997. Annu. Rev. Astron. Astrophys. 35:309
10. Foley, RJ, Berger E, Fox O, Levesque EM, Challis PJ, Ivans II, et al. 2011, ApJ, 732, 32
11. Foley RJ, Smith N, Ganeshalingam M, Li W, Chornock R, Filippenko AV. 2007, ApJL, 657, L105
12. Fox O, Skrutskie MF, Chevalier RA, Kanneganti S, Park C, Wilson J, et al. 2009, ApJ, 691, 650
13. Fransson C, Ergon M, Challis PJ, Chevalier RA, France K, Kirshner RP, et al., 2014, ApJ, 797, 118
14. Fraser M, Inessa C, Jerkstrand A, Kotak R, Pignata G, Benetti S, et al. 2013a, MNRAS, 433, 1312
15. Fraser M, Magee M, Kotak R, Smartt SJ, Smith KW, Polshaw J, et al. 2013b, ApJ, 779, L8
16. Gall C, Hjorth J, Watson D, Dwek E, Maund JR, Fox O, et al. 2014, Nature, 511, 326
17. Gal-Yam, A, Leonard DC, Fox DB, Cenko SB, Soderberg AM, Moon DS, et al. 2007, ApJ, 656, 372
18. Gal-Yam A, & Leonard DC. 2009, Nature, 458, 865
19. Gal-Yam A, Arcavi I, Ofek EO, Ben-Ami S, Cenko SB, Kasliwal MM, et al. 2014, Nature, 509, 471
20. Gehrz RD, Hackwell JA. 1974, ApJ, 194, 619
21. Kochanek CS, Szczygiel DM, & Stanek KZ. 2011, ApJ, 737, 76
22. Leonard DC, Filippenko AV, Barth AJ, Matheson T. 2000, ApJ, 536, 239
23. Margutti R, Milisavljevic D, & Soderberg AM. 2014, ApJ, 780, 21
24. Matheson T, Filippenko AV, Barth AJ, Ho LC, Leonard DC, Bershadsky MA, et al. 2000, AJ, 120, 1487
25. Mauerhan JC, Smith N, Filippenko AV, Blanchard KB, Blanchard PK, Casper CFE, et al. 2013a, MNRAS, 430, 1801
26. Mauerhan JC, Smith N, Silverman JM, Filippenko AV, Morgan AN, Cenko SB, et al. 2013b, MNRAS, 431, 2599
27. Mauerhan JC, Williams GG, Smith N, Smith PS, Filippenko AV, Hoffman JL, et al. 2014, MNRAS, 442, 1166
28. Meakin C, Arnett WD. 2007, ApJ, 667, 448
29. Milisavljevic D, & Fesen RA. 2013, ApJ, 772, 134
30. Miller A, Silverman JM, Butler NR, Bloom JS, Chornock R, Filippenko AV, et al. 2010, MNRAS, 404, 305
31. Niemela VS, Ruiz MT, Phillips MM. 1985, ApJ, 289, 52

32. Nomoto K, Sugimoto D, Sparks WM, Fesen RA, Gull TR, Miyaji S. 1982, *Nature*, 299, 803
33. Ofek EO, Cameron PB, Kasliwal MM, Gal-Yam A, Rau A, Kulkarni SR, et al. 2007, *ApJ*, 659, L13
34. Ofek EO, Lin L, Kouveliotou C, Younes G, Gogus E, Kasliwal MM, Cao Y. 2013a, *ApJ*, 768, 47
35. Pastorello A, Smartt SJ, Mattila S, Eldridge JJ, Young D, Itagaki K, et al. 2007, *Nature*, 447, 829
36. Pastorello A, Mattila S, Zampieri L, Della Valle M, Smartt SJ, Valenti S, Agnoletto I, et al. 2008, *MNRAS*, 389, 113
37. Pastorello A, Cappellaro E, Inerra C, Smartt SJ, Pignata G, Benetti S, et al. 2013, *ApJ*, 767, 1
38. Pastorello A, Benetti S, Brown PJ, Tsvetkov DY, Inerra C, Taubenberger S, et al. 2015, *MNRAS*, 449, 1921
39. Pozzo M, Meikle WPS, Fassia A, Geballe T, Lundqvist P, Chugai NN, et al. 2004, *MNRAS*, 352, 457
40. Prieto JL, Brimacombe J, Drake AJ, Howerton S. 2013, *ApJL*, 763, L27
41. Rest A, Foley RJ, Gezari S, Narayan G, Draine B, Olsen K, et al. 2011, *ApJ*, 729, 88
42. Roming PWA, Pritchard TA, Prieto JL, Kochanek CS, Fryer CL, Davidson K, et al. 2012, *ApJ*, 751, 92
43. Quataert E, Shiode J. 2012, *MNRAS*, 423, L92
44. Sana H, de Mink SE, de Koter A, Langer N, Evans CJ, Gieles M, et al. 2012, *Sci*, 337, 444
45. Schlegel EM. 1990, *MNRAS*, 244, 269
46. Shivvers I, Mauerhan JC, Leonard DC, Filippenko AV, Fox OD. 2015, *ApJ*, 806, 213
47. Silverman JM, Nugent PE, Gal-Yam A, Sullivan M, Howell DA, et al. 2013, *ApJ Suppl.*, 207, 3
48. Smartt SJ. 2009, *ARA&A*, 47, 63
49. Smith N. 2013, *MNRAS*, 434, 102
50. Smith N. 2014, *ARA&A*, 52, 487
51. Smith N, Arnett WD. 2014, *ApJ*, 785, 82
52. Smith N, Li W, Foley RJ, Wheeler JC, Pooley D, Chornock R, et al. 2007, *ApJ*, 666, 1116
53. Smith N, Chornock R, Li W, Ganeshalingam M, Silverman JM, Foley RJ, et al. 2008a, *ApJ*, 686, 467
54. Smith N, Foley RJ, Filippenko AV. 2008b, *ApJ*, 680, 568
55. Smith N, Silverman JM, Chornock R, Filippenko AV, Wang X, et al. 2009, *ApJ*, 695, 1334
56. Smith N, Chornock R, Silverman JM, Filippenko AV, Foley RJ. 2010a, *ApJ*, 709, 856
57. Smith N, Miller A, Li W, Filippenko AV, Silverman JM, Howard AW, et al. 2010b, *AJ*, 139, 1451
58. Smith N, Li W, Filippenko AV, Chornock R. 2011a, *MNRAS*, 412, 1522
59. Smith N, Li W, Silverman JM, Ganeshalingam M, Filippenko AV. 2011b, *MNRAS*, 415, 733
60. Smith N, Mauerhan JC, Silverman JM, Ganeshalingam M, Filippenko AV, Cenko SB, et al. 2012, *MNRAS*, 426, 1905
61. Smith N, Silverman JM, Filippenko AV, Cooper MC, Matheson T, Bian F, et al. 2012, *AJ*, 143, 17
62. Smith N, Mauerhan JC, Prieto JL. 2014, *MNRAS*, 438, 1191
63. Smith N, Mauerhan JC, Cenko SB, Kasliwal MM, Silverman JM, Filippenko AV, et al., 2015, *MNRAS*, 449, 1876
64. Stritzinger M, Taddia F, Fransson C, Fox OD, Morrell N, Phillips MM, et al. 2012, *ApJ*, 756, 173
65. van Marle AJ, Smith N, Owocki SP, van Veelen B. 2010, *MNRAS*, 407, 2305
66. Williams PM, van der Hucht KA, Pollock AMT, Florkowski DR, van der Woerd H, Wamsteker WM. 1990, *MNRAS*, 243, 662
67. Woosley SE, Blinnikov S, Heger A. 2007, *Nature*, 450, 390
68. Yoon SC, Cantiello M. 2010, *ApJ*, 717, L62